PERGAMON

International Journal of Heat and Mass Transfer 45 (2002) 543–553

International Journal of HEAT and MASS TRANSFER

www.elsevier.com/locate/ijhmt

Heat transfer and pressure drop for low Reynolds turbulent flow in helically dimpled tubes

Pedro G. Vicente *, Alberto García, Antonio Viedma

Department of Thermal and Fluids Engineering, Technical University of Cartagena, Paseo Alfonso XIII 48, 30203 Cartagena, Spain

Received 10 August 2000; received in revised form 30 April 2001

Abstract

Three-dimensional helically dimpled tubes have been experimentally studied in order to obtain their heat transfer and isothermal friction characteristics. Using water and ethylene glycol as test fluids, a wide range of fluid flow conditions was covered: $2000 < Re < 100{,}000$ and $2.5 < Pr < 100$. An experimental study of 10 tubes with different geometric forms (dimple height h/d ranging from 0.08 to 0.12 and helical pitch p/d, from 0.65 to 1.1) offers insight into the influence of manufacturing parameters on tube thermohydraulic behaviour. The large amount of experimental data have been correlated so as to obtain easy to use expressions for Fanning friction factors and Nusselt numbers as functions of flow and geometry non-dimensional parameters. Performance evaluation criteria, commonly used in the enhanced heat transfer literature, were calculated in order to assess the real benefits offered by dimpled tubes.

1. Introduction

Heat transfer enhancement through artificial roughness is an interesting current technique for obtaining compact and more efficient heat exchangers. Tubes with inside roughness can reduce size and cost of the equipment and are successfully used in practical applications. There are two tube-side artificial roughness methods: two-dimensional roughness (transverse and helical ribs, helically corrugated and wire coil inserts) and three-dimensional roughness (sand-grain roughness, attached particle roughness, "cross-rifled" roughness and helically dimples). Only tubes with artificial roughness obtained by cold rolling the external tube surface are used in practical applications: corrugated, helically ribbed and helically dimpled tubes.

Substantial work has been carried out on corrugated and helically ribbed tubes and several design correlations are available for commercial tubes. However, very little experimental data relating to helically dimpled tubes has been published. Therefore, it is difficult to use these tubes in heat exchanger design.

Enhanced tubes can be used for many applications, like evaporators, condensers, oil refrigerators and heat exchangers for sterilising processes. The present study is focused on improving heat exchangers used for sterilising organic fluids, through helically dimpled tubes.

In heat exchangers for sterilising fluids, organic fluid flows through tubes and is heated by steam or hot water flowing on the outside. Flow conditions at the outer fluid flow area usually reach high Reynolds numbers, and the outside film coefficient h_o is therefore relatively high. However, organic fluids usually present high viscosity and inside flow can either be laminar or turbulent at low Reynolds numbers. The inside film coefficient h_i is thus relatively small.

The inside film coefficient is often much smaller than the outside one ($h_i \ll h_o$) and it becomes the critical value in the overall heat transfer coefficient ($U \approx h_i$). In order to increase the heat duty Q of these heat exchangers, the effort should be focused on increasing the inside film coefficient h_i.

Interior roughness increases heat transfer by mixing the flow in the boundary layer and also by increasing the turbulence level of the fluid flow. This perturbation in the flow causes an undesirable increasement of pressure drop. Heat transfer and pressure drop variations must be analysed to check the real benefits of enhanced tubes.

* Corresponding author.
E-mail address: Pedro.Vicente@upct.es (P.G. Vicente).

0017-9310/02/$ - see front matter
PII: S0017-9310(01)00170-3

Nomenclature

A	heat transfer area ($\pi d l_h$) (m^2)
c_p	specific heat of the test fluid (J kg^{-1} K^{-1})
d	envelope (maximum inside) diameter (m)
h	roughness height (Fig. 2) (m)
h^+	roughness Reynolds number $(h/d)Re\sqrt{f/2}$
h_o	outside heat transfer coefficient (W m^{-2} K^{-1})
h_i	inside heat transfer coefficient (W m^{-2} K^{-1})
I	intensity (A)
k	thermal conductivity (W m^{-1} K^{-1})
l	length between dimples (Fig. 2) (m)
l_p	length of test section between pressure taps (m)
l_h	length of the heat transfer section (m)
$\dot{m}$	mass flow rate of the test fluid (kg s^{-1})
p	helical pitch (Fig. 2) (m)
ΔP	pressure drop across the test section (N m^{-2})
P	pumping power (W)
Q	heat transfer rate (W)
q''	heat flux ($VI/\pi d l_n$) (W m^{-2})
t	temperature (K)
t_{wi}	inside surface temperature of the wall (K)
t_{wo}	outside surface temperature of the wall (K)
V	voltage (V)
U	overall heat transfer coefficient (W m^{-2} K^{-1})
v	average velocity of the fluid (m s^{-1})

Dimensionless groups

f	Fanning friction factor ($\Delta P d/2\rho v^2 l_p$)
$G(h^+, Pr)$	heat transfer roughness function
Nu	Nusselt number ($h_i d/k$)
Pr	Prandtl number ($c_p \mu/k$)
Re	Reynolds number ($\rho v d/\mu$)
$R(h^+)$	momentum transfer roughness function
St	Stanton number ($Nu/RePr$)

Greek symbols

μ	dynamic viscosity (kg m^{-1} s^{-1})
ρ	fluid density (kg m^{-3})

Subscripts

a	augmented tube (dimpled tube)
b	based on bulk temperature
in	tube inlet
out	tube outlet
s	smooth tube
w	based on wall temperature
x	local value

The aim of this study was to obtain experimental data from in-tube one-phase turbulent flow of dimpled tubes between Reynolds numbers $2000 < Re < 100{,}000$ and Prandtl numbers $2.5 < Pr < 100$. A number of performance evaluation criteria suggested by Bergles et al. [1] have been used to realistically estimate the benefits offered by helically dimpled tubes for heat exchangers.

2. Background

This section discusses different studies on three-dimensional roughness. Three-dimensional roughness holds interest because of the high levels of enhancement and energy efficiency that can be obtained from its use, compared to levels obtained by other passive enhancement geometric forms [2]. In fact it turns out to be one of the best types of surface modifications for improving heat transfer performance in one phase turbulent forced convective flows.

- Cope [3] was the first to study three-dimensional roughness. He analysed roughness produced by knurling the inner tube surface.
- Dipprey and Sabersky [4] studied tube surfaces having a close-packed sand-grain-type roughness, which resembles natural roughness because of its three-dimensional nature and the random shape of the roughness elements.
- Takahashi et al. [5], and afterwards Guanga et al. [6], studied three dimensional internally finned tubes made by rolling copper tubes using internal mandrels.

These types of roughness are not suitable for many of the practical applications, due to the high cost of roughness generating procedures. Only helically dimpled tubes – for which dimples on the inner surface are formed by rolling spaced protrusions on the outer surface – are actually implemented in practical applications at a reduced cost.

- Kuwahara et al. [7] registered a US Patent for spirally dimpled tubes. They tested 7 tubes within the following geometric ranges: $0.028 < h/d < 0.038, 0.32 < p/d < 0.64$ and $0.16 < l/d < 0.32$. They assessed thermal and hydraulic performance in water with $5000 < Re < 100{,}000$ and $Pr \approx 5$.
- Rabas et al. [8] tested two helically dimpled tubes with small dimples like the Tred-19F and Tred-26D tested by Sumitomo (reported by Webb [2]). Dimple height was $h/d = 0.017$, and pitch was $p/d = 0.18$ and 0.09 (for one and two rows of dimples, respectively). Flow range was $6000 < Re < 70{,}000$

and $Pr = 5.7$. They obtained a very good agreement between their experimental data and predicted values, numerically obtained over the discrete-element method developed by Taylor and Hodge [9].

- Olsson and Sundén [10] studied the thermal and hydraulic performance of five dimpled tubes made by rolling two, three or four rows of dimples on the outer surface. The focus was on determining the friction coefficient and Nusselt number in small tubes for radiators. The little published data relating to three-dimensional dimpled tubes hinders their implementation. The current paper is a contribution to experimental data relating to three-dimensional roughness generated through dimples formed by rolling the outer surface. The geometric range covered is $0.08 < h/d < 0.12, 0.65 < p/d < 1.1$ and $l/d \approx 0.55$, whereas the turbulent flow range lies within $2000 < Re < 100{,}000$ and $2.5 < Pr < 100$. Fig. 1 shows the aspect ratio map (h/d vs. p/d) covered in this paper, compared to the above references.

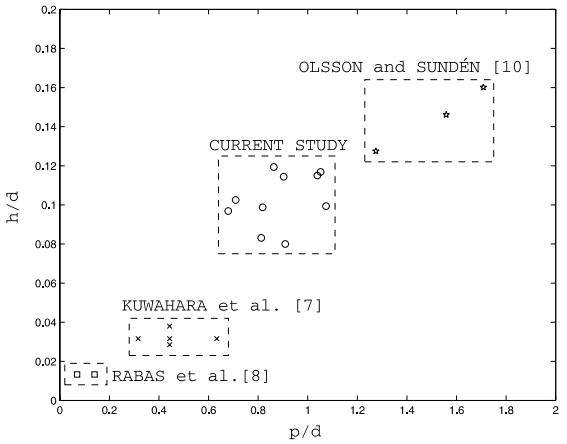

Fig. 1. Aspect ratio map for helically dimpled tubes.

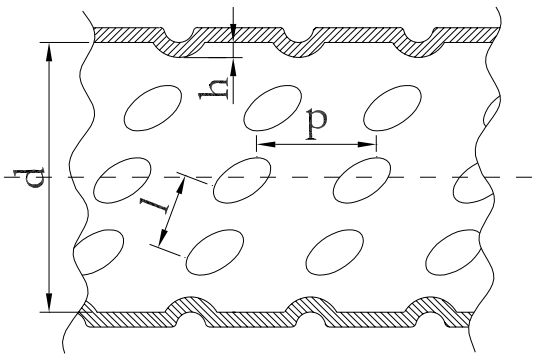

Fig. 2. Sketch of a dimpled tube.

3. Experimental program

3.1. Tested tubes

10 helically dimpled tubes of different geometric forms and one smooth tube were studied in the experiment. All tubes had inside diameters of $d = 16$ mm with a wall thickness of 1 mm before the cold rolling operation. The smooth tube was used for checking and adjusting the experimental set-up and also for comparing the enhancement obtained by dimpled tubes. All enhanced tubes were fabricated from plain stainless steel 316L tube and were plastically deformed by rolling spaced protrusions on the outer surface.

Fig. 2 shows a sketch of a dimpled tube, where p stands for helical pitch; h, dimple height; and l, distance between dimples. Two non-dimensional parameters have been used to define tube roughness: reduced height h/d and dimple density d^2/pl.

The inside diameter d is the envelope diameter defined by Bergles et al. [1] which is the maximum inside diameter. This diameter will be used as a length scale for Re, Nu and f. This approach is recommended by Marner et al. [11] since it allows for performance comparison between two enhanced tubes and also between an enhanced tube and a smooth one.

The above parameters describing the tubes geometry are listed in Table 1.

Table 1
Geometry of tested tubes

Tube no	d (mm)	h (mm)	p (mm)	l (mm)	h/d	d^2/pl
01	16.0	1.33	13.0	8.85	0.0831	2.225
02	16.0	1.58	13.1	8.99	0.0988	2.175
03	16.0	1.91	13.8	8.89	0.1194	2.085
04	16.0	1.28	14.6	8.91	0.0800	1.975
05	16.0	1.83	14.5	9.02	0.1144	1.964
06	16.0	1.59	17.2	9.02	0.0994	1.652
07	16.0	1.84	16.6	9.06	0.1150	1.700
08	16.0	1.87	16.8	8.90	0.1169	1.709
09	16.0	1.55	10.9	8.90	0.0969	2.646
10	16.0	1.64	11.4	8.76	0.1025	2.575

3.2. Test fluids

To extend Reynolds number range, two different fluids were used: water and ethylene glycol. Reynolds number range comprises 2000–10,000 for ethylene glycol and 8000–100,000 for water. Prandtl number range covers from 35 to 100 for ethylene glycol and 2.9–4.5 for water.

3.3. Experimental set-up

Heat transfer experiments were carried out under constant heat flux conditions ($q'' = \text{cte}$). Energy was added to the working fluid by alternating current Joule heating . Pressure drop tests were done with no heat addition (isothermal conditions).

A sketch of the experimental set-up is shown in Fig. 3. The test circuit consisted of a variable-speed centrifugal pump, an oval wheels flowmeter and the test section. The test fluid was pumped from an open reservoir tank and then passed through the flowmeter into the test section. There, it was heated and returned to the tank.

The actual test section is consists of a 1-m long stainless steel tube heated by a 6 KVA transformer. The transformer was connected to an autotransformer so as to regulate power supply. The tube wall was heated by Joule effect and energy was added to the working fluid through the inner wall. Maximum heat loss was about 0.5% since the tube was highly insulated.

To keep a constant temperature in the tank, a cooling circuit was added. This secondary loop consisted of a variable-speed centrifugal pump, a double-pipe heat exchanger and an electrical heater. The fluid was cooled by chilled water in the counterflow heat exchanger. The electrical heater, controlled by a PID, allowed for adjusting the temperature in the tank to the desired value.

All temperatures were measured by resistive temperatures devices (RTDs). "A" class RTDs connected by four wires to an HP 34970A Data Acquisition Unit, ensured 0.08°C accuracy . Fluid inlet and outlet temperatures t_{in}, t_{out} were measured by submerged type RTDs. Outside wall temperature was measured at one axial position by eight accurate RTDs spaced 45°. The RTDs were fixed on the outer surface by a high thermal conductivity adhesive. A calibration test with no energy addition was done previous to every test in order to calibrate layout resistance.

Overall electrical power added to the fluid, Q, was calculated by measuring voltage (0–15 V) and current (0–600 A). Fluid outlet temperature t_{out} can be indirectly calculated by an energy balance

$$t_{out} = t_{in} + \frac{Q}{\dot{m}c_p}. \tag{1}$$

The difference between fluid outlet temperature t_{out} measured and the one calculated by Eq. (1) was in every instance less than 0.1°C.

Since heat was homogeneously added across the tube wall, the mean temperature of the flow linearly varies along the axial direction of x. Bulk temperature of the fluid at any x location in the tube is given by the expression

$$t_b(x) = \frac{t_{out} - t_{in}}{l_h} x + t_{in}. \tag{2}$$

Heat flux q'' is defined by

$$q'' = \frac{Q}{\pi d l_h} = \frac{VI}{\pi d l_h}. \tag{3}$$

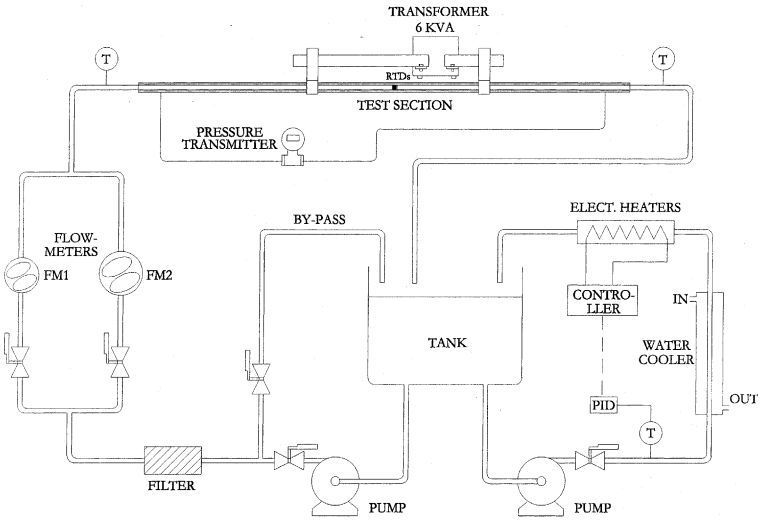

Fig. 3. A schematic diagram of the experimental set-up.

Nusselt number was calculated using the expression

$$Nu(x) = \frac{d}{k}\frac{q''}{(t_{wi}(x) - t_b(x))}, \quad (4)$$

where t_{wi} is the mean temperature of the inner wall. The mean temperature of the outer wall t_{wo} was calculated as the mean value of the eight wall RTDs measurements placed on the same section. The mean temperature of the inner wall t_{wi} was numerically calculated by solving the steady-state one-dimensional heat conduction equation with heat generation in the tube wall.

Nusselt numbers calculated by Eq. (4) were corrected by a factor that takes fluid viscosity at the boundary layer into account. A set of experiments showed that factor $(\mu_b/\mu_w)^{-0.14}$ corrected the mentioned effect. The 0.14 exponent was used in Sieder–Tate equation and by Sethumadhavan and Rao [12] and results varied little with respect to the more widely used 0.11 exponent, proposed by Kays and Crawford [13].

In turbulent flow, even for low Reynolds numbers, flow is fully developed at $x/d = 15$ [14]. The local Nusselt number was determined on a section located at $x/d = 35$ and therefore this is the asymptotic Nusselt number. The entry region under turbulent flow is very small. If the tube is not short, it can be neglected. Therefore it can be assumed that the calculated asymptotic Nusselt number is approximately the mean Nusselt number.

The heat transfer tests were carried out at five different Prandtl numbers: 92, 59, 37, 4.2 and 2.9, working with ethylene glycol at 40°C, 55°C and 70°C and water at 40°C and 60°C. Prandtl number remained constant during the test, run keeping fluid mean temperature constant at the measure point. Tank temperature was regulated for every measurement in order to have the desired temperature at the measure point.

Isothermal pressure drop studies were done with water at 25°C and 55°C and ethylene glycol at 55°C to cover a continuous Reynolds number range from 2000 to 100,000. Fanning friction coefficients were determined from fluid flow rate and pressure drop measurements. A highly accurate pressure transmitter was used to measure the pressure drop along a 5.2 m tube length.

3.4. Experimental uncertainty

Experimental uncertainty was calculated following Kline and McClintock [15] method based on a 95% confidence level. Instrumentation errors were as follows: temperature, 0.08°C; flow rate, 0.4% f.s.; differential pressure 0.075% span; intensity 0.1% measure + 0.04% f.s.; and voltage, 0.04% measure + 0.03% f.s. The thermophysical properties of the tested fluids have been assigned an uncertainty of ±0.5% to ρ and ±1% to μ, c_p and k. An uncertainty of 0.1% has been allocated to the inner diameter of the test tube. Test section length uncertainties were 5 mm for the pressure test section and 10 mm for the heat transfer test section.

Uncertainty calculations showed maximum values of 4% for Reynolds number, 3.5% for Prandtl number, 3% for friction factor and 4.5% for Nusselt number.

4. Results and discussion

4.1. Pressure drop

Isothermal pressure drop studies were performed for water and ethylene glycol in the range between $Re = 200$ and 100,000 in smooth and dimpled tubes. Only results for the turbulent region ($2000 < Re < 100{,}000$) are discussed in this paper. Pressure drop results for the laminar and transitional region will be shown in a future paper.

The experimental set-up was checked and adjusted through pressure drop experiments with a smooth tube. Pressure-drop data, collected under isothermal conditions within a Reynolds number range 2000–100,000, were compared to Blasius equation

$$f_s = 0.0791\,Re^{-0.25}. \quad (5)$$

Friction factor data predictions were in agreement with the smooth tube correlation, within a deviation of 3% for 95% of the experimental data.

Pressure-drop test data for the 10 dimpled tubes were reduced and results are plotted as Fanning friction factors in Fig. 4. Turbulent flow friction factors measured

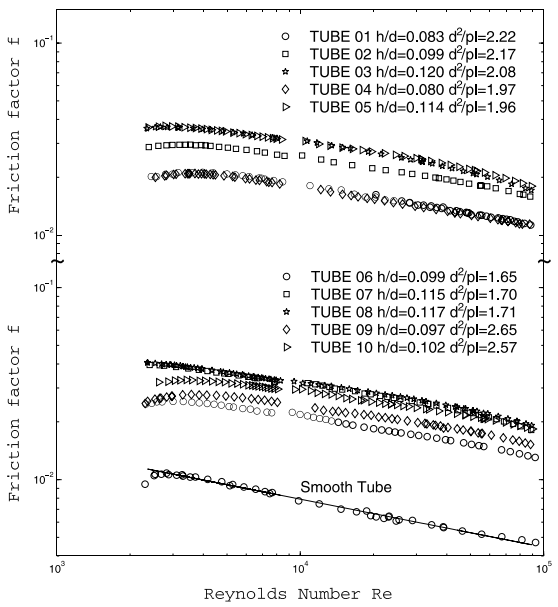

Fig. 4. Friction factor vs. Reynolds number.

for dimpled tubes were significantly higher than those in the smooth tube. Enhanced tube friction factors are 2–4.5 times higher than those for a smooth tube (Fig. 5).

The friction data points for each tube define a continuous curve. The following three regions can be delimited:

1. From transition to $Re \approx 4000$. In this region, the friction factor presents a maximum.
2. From $Re \approx 4000$ to $Re \approx 40{,}000$. Friction curves for all the tubes decrease with the increase of Re, under a constant relation: $f_a \propto Re^{-0.19}$.
3. From $Re \approx 40{,}000$ to $Re \approx 100{,}000$. The slope in the curve for the friction factor changes.

Friction factors for all tubes were correlated in the Re range between 4000 and 40,000. The correlation developed is a function of reduced height h/d and dimple density d^2/pl:

$$f_a = 5.52(h/d)^{1.67}(d^2/pl)^{0.26}Re^{-0.19}. \quad (6)$$

Eq. (6) predicts the friction factor data to be under 10% for 95% of the experimental data. This correlation shows a strong influence of dimpled height on the friction factor, whereas dimple density has a smaller influence. Friction augmentation (f_a/f_s) can be calculated by dividing Eq. (6) by Eq. (5)

$$f_a/f_s = 69.9(h/d)^{1.67}(d^2/pl)^{0.26}Re^{0.06}. \quad (7)$$

Friction factor results in dimpled tubes were also analysed in terms of momentum transfer roughness function $R(h^+)$ and roughness Reynolds number h^+. Nikuradse [16] developed the friction similarity law for sand-grained tubes, which has successfully been used for correlating friction results for artificial roughness surfaces. The roughness function is defined by:

$$R(h^+) = \sqrt{2/f_a} + 2.5\ln(2h/d) + 3.75, \quad (8)$$

and roughness Reynolds number by $h^+ = h/dRe\sqrt{2/f_a}$.

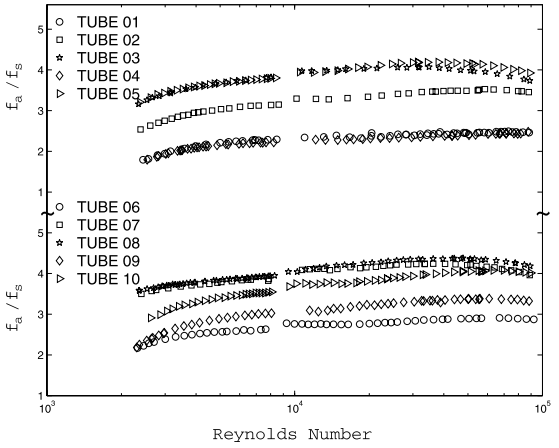

Fig. 5. Friction factor increase f_a/f_s vs. Reynolds number.

Fig. 6 shows the momentum transfer roughness function $R(h^+)$ as a function of roughness Reynolds number h^+ for all tested tubes. The figure shows that the roughness function does not depend only on h^+, but also on roughness geometry. This fact was reported by Webb et al. [17] for transverse-rib roughness and by Sethumadhavan and Rao [12] for corrugated for corrugated tube roughness.

The friction factor for all tubes was correlated with h^+ ranging from 70 to 500. The resulting correlation is a function of reduced height h/d, dimple density d^2/pl and roughness Reynolds number h^+.

$$R(h^+) = 0.839(h/d)^{-0.85}(d^2/pl)^{-0.18}(h^+)^{0.11}. \quad (9)$$

Eq. (9) predicts $R(h^+)$ data within 5% for 95% of the experimental data. This error in $R(h^+)$ produces a $\pm 10\%$ deviation for the friction factor prediction.

As shown in Fig. 4 and in Eq. (6), friction factor decreases alongside Reynolds number. This result was also obtained for dimpled tubes by Kuwakara et al. [7] and Olsson and Sundén [10]. In sand grain roughened tubes, Nikuradse [16] and Dipprey and Sabersky [4] found constant friction factors for the fully rough condition ($h^+ > 70$).

In two-dimensional roughness, Webb et al. [17] also observed a constant friction factor at high Reynolds numbers for tubes with repeated-rib roughness. Experimental studies on corrugated tubes [12,18] showed a decrease in friction factor alongside Reynolds number. Zimparov et al. [18] friction factor results for 25 spirally corrugated brass tubes offered $f \propto Re^{-0.10}$ to $Re^{-0.16}$ (smaller than those obtained by us: $f \propto Re^{-0.19}$). Recent experimental results by Brognaux et al. [19] for micro-fin tubes showed a similar friction factor slope $f \propto Re^{-0.20}$ for their "MX" tubes. Sethumadhavan and

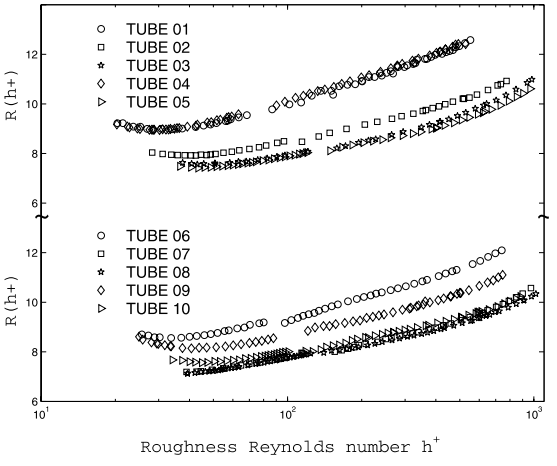

Fig. 6. Momentum roughness function $R(h^+)$ vs. roughness Reynolds number h^+.

Rao [12] correlated their experimental data using the momentum roughness function, resulting in $R(h^+) \propto (h^+)^{0.16}$, a little higher than $R(h^+) \propto (h^+)^{0.11}$ shown in Eq. (9).

4.2. Heat transfer

Heat transfer studies under constant heat flux conditions were carried out for both the smooth and all dimpled tubes. In order to cover a wide Reynolds and Prandtl range, each tube was tested with water and ethylene glycol at different temperatures. Experiments with ethylene glycol were carried out at 40°C, 55°C and 70°C which corresponds to Prandtl numbers of 92, 59 and 37, covering a Reynolds number range $Re = 2000$–$10{,}000$. Water tests were carried out at Prandtl numbers $Pr = 4.1$ and 2.9 (40°C and 65°C) and a Reynolds number range $Re = 10{,}000$–$100{,}000$.

Smooth tube results for ethylene glycol were compared with the correlation proposed by Gnielinski [20].

$$Nu_s = \frac{(f_s/2)(Re - 1000)Pr}{1 + 12.7\sqrt{f_s/2}(Pr^{2/3} - 1)}. \quad (10)$$

The data measured are higher than those predicted by Gnielinski's equation within a range 2–9%.

Smooth tube results for water agreed within ±4% to Petukhov's [21] correlation:

$$Nu_s = \frac{(f_s/2)RePr}{1.07 + 12.7\sqrt{f_s/2}(Pr^{2/3} - 1)}, \quad (11)$$

where the friction factor f_s for Eqs. (10) and (11) is given by $f_s = (1.58 \ln Re - 3.28)^{-2}$.

Fig. 7 shows the results for the smooth tube compared to Eqs. (10) and (11). A single correlation covering the whole range ($2000 < Re < 100{,}000$ and $2.9 < Pr < 92$) was drawn to correlate Nusselt number results,

$$Nu_s = 0.0167(Re - 1000)^{0.84}Pr^{0.4}. \quad (12)$$

This equation correlates the experimental Nusselt number for the smooth tube with a deviation within ±3%, and was used to evaluate heat transfer augmentation of dimpled tubes.

Turbulent flow heat transfer experiments were carried out for the 10 dimpled tubes described in Table 1 About 60 experimental points were set for each tube in order to determine Re and Pr influence on Nu_a. Measurements were taken at 5 fixed Prandtl numbers: 2.9, 4.1, 37, 59 and 92. Fig. 8, as an example of the measurements, shows Nu_a vs. Re experimental results for the different Prandtl numbers from Tube 03. The tubes tested are assumed to be geometrically similar. Therefore, a Nusselt number equation in the the form $Nu_a = Nu_a(Re, Pr, h/d, d^2/pl)$ can be obtained, in order to characterise the tube family. The following general correlation was obtained via curve-fitting:

$$Nu_a = 1.07(h/d)^{0.69}(d^2/pl)^{0.12}(Re - 1000)^{0.63}Pr^{0.4}. \quad (13)$$

This equation correlates 95% of the experimental data within ±7%.

Eq. (13) shows Prandtl number's influence on heat transfer ($Nu_a \propto Pr^{0.4}$). This relation is the same for the smooth tube; therefore, heat transfer enhancement produced by dimpled tubes is not a function of the Prandtl number.

Fig. 9 shows the heat transfer results plotted as $Nu_aPr^{-0.4}$ vs. Re, for the smooth and the 10 dimpled tubes. Reduced height h/d is the geometric parameter that has the strongest influence on Nu_a.

The $(Re - 1000)$ coefficient is lower than the smooth tube correlation (Eq. (12)). Therefore, Nusselt number augmentation decreases with Re, $(Nu_a/Nu_s) \propto (Re - 1000)^{-0.21}$. Fig. 10 shows Nusselt number increase (Nu_a/Nu_s vs. Re) for the 10 dimpled tubes tested by us.

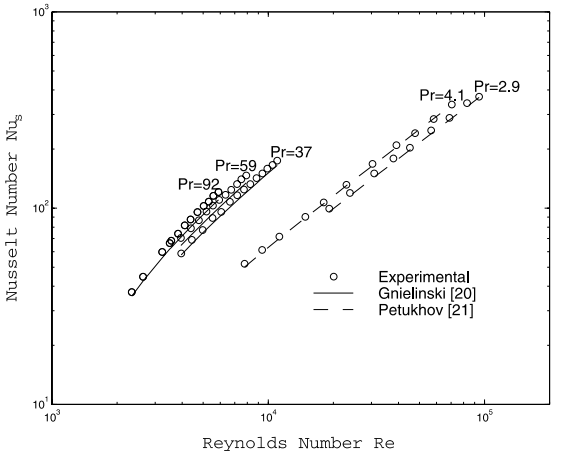

Fig. 7. Nusselt number vs. Reynolds number. Smooth tube.

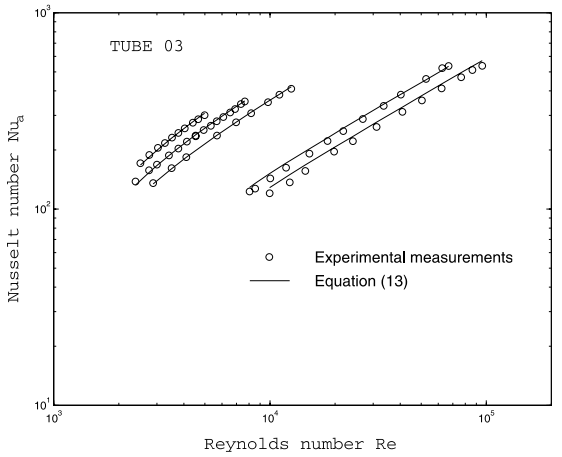

Fig. 8. Nusselt number vs. Reynolds number. Tube 03.

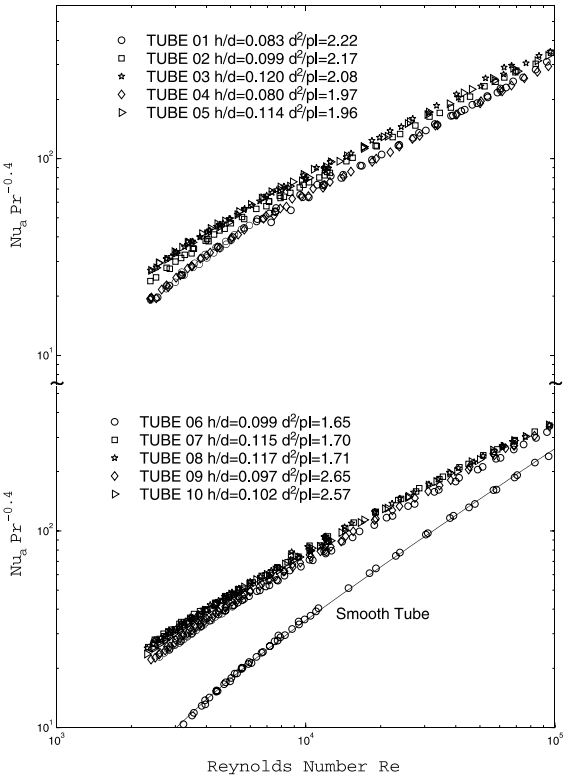

Fig. 9. Heat transfer results for the dimpled tubes. $NuPr^{-0.4}$ vs. Re.

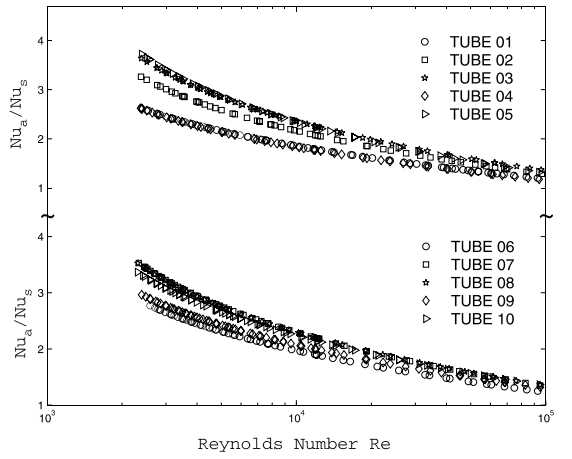

Fig. 10. Nusselt number increase Nu_a/Nu_s vs. Reynolds number.

Heat transfer results were also analysed in terms of the heat transfer roughness function $G(h^+, Pr)$. Dipprey and Sabersky [4] developed the concept of heat transfer roughness function $G(h^+, Pr)$. This function was first used by Webb et al. [17] and later by many other authors to analyse their experimental data from artificial roughness surfaces. The heat transfer roughness function is assumed to be written as the product of $G(h^+)Pr^n$

$$G(h^+)Pr^n = \frac{f_a/(2\mathrm{St}) - 1}{\sqrt{f_a/2}} + R(h^+). \tag{14}$$

Fig. 11 shows the heat transfer roughness function $G(h^+, Pr)$ as a function of roughness Reynolds number h^+. Prandtl number dependence was found to be $G(h^+, Pr) \propto Pr^{0.6}$. Fig. 12 shows that experimental results in the form $G(h^+)Pr^{-0.6}$ vs. h^+ were accurately correlated. Reduced height h/d, and dimple density d^2/pl do not have any influence on $G(h^+)$. The influence of these geometrical parameters on heat transfer is included in the friction factor f_a and in the roughness function $R(h^+)$, (Eq. (14)).

The following general correlation for $G(h^+)$ is proposed:

$$G(h^+)Pr^{-0.60} = 4.871(h^+)^{0.24}. \tag{15}$$

This equation along with Eq. (9) for $R(h^+)$ yields to a deviation in the calculated Nusselt number within $\pm 7.5\%$ in the range $65 < h^+ < 1000$. For $20 < h^+ < 65$,

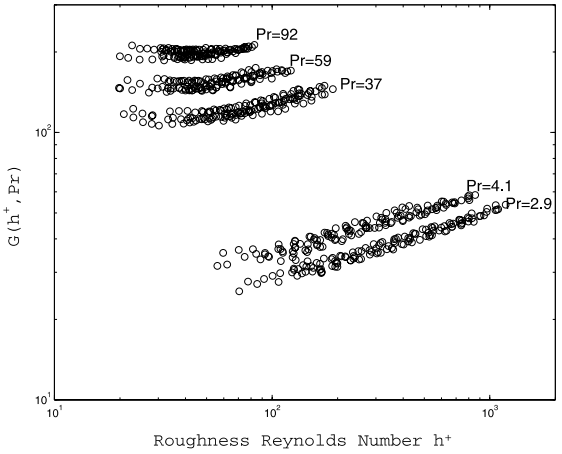

Fig. 11. Heat transfer roughness function $G(h^+, Pr)$ vs. roughness Reynolds number h^+.

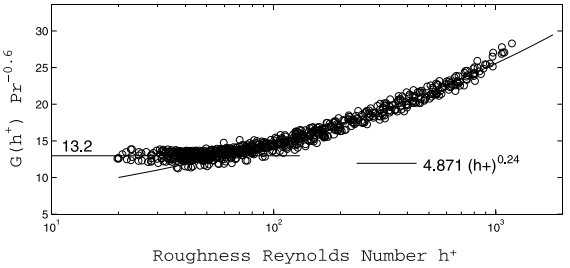

Fig. 12. $G(h^+)Pr^{-0.6}$ vs. roughness Reynolds number h^+.

the heat transfer roughness function is constant $G(h^+) = 13.2$.

Experimental results show that – for dimpled tubes – Nusselt number enhancement Nu_a/Nu_s decreases with Reynolds number. This effect was also reported by Kuwakara et al. [7] and Olsson and Sundén [10] for three-dimensional helically dimpled tubes. Heat transfer predictions of Rabas et al. [8], who employed Taylor and Hodge [9] method, lead to a maximum Nu_a/Nu_s at $h^+ \approx 35$–60.

The proposed heat transfer roughness function $G(h^+, Pr)$ can be compared to those proposed in other papers relating to two-dimensional roughness. Prandtl number's influence $G(h^+) \propto Pr^{0.60}$ is slightly higher than the one obtained by Webb et al. [17] ($G(h^+) \propto Pr^{0.57}$) or Sethumadhavan and Rao [12] ($G(h^+) \propto Pr^{0.55}$). On the other hand, roughness Reynolds number's influence was $G(h^+) \propto (h^+)^{0.24}$ which agrees with the ones obtained by Webb et al. [17] ($G(h^+) \propto (h^+)^{0.28}$) for repeated-rib roughness and by Dipprey and Sabersky [4] ($G(h^+) \propto (h^+)^{0.20}$) for sand-grained roughness.

5. Performance evaluation

Bergles et al. [1] and Webb [22] proposed several performance criteria to technically evaluate the thermohydraulic performance of enhanced tubes. In this paper, Criterias R1, R3 and R5 outlined by Bergles et al. [1] were assessed to verify the real benefits from dimpled tubes. These three criteria compare the augmented tube to the smooth one in the following way:

- Criterion R1: Assesses heat transfer rate for equal flowrates and surface areas ($\dot{m}_s/\dot{m}_a = 1, A_s/A_a = 1$).
- Criterion R3: Assesses heat transfer rate for equal pumping powers and heat exchange surface areas ($P_s/P_a = 1, A_s/A_a = 1$).
- Criterion R5: Assesses reduction of tube surface area for equal pumping powers and heat duties ($P_s/P_a = 1, Q_s/Q_a = 1$).

Performance ratios were evaluated using h_a/h_s, assuming a very small ratio between (a) combined outside film and metal wall resistances and (b) inside film resistance. Thus $U_a/U_s \approx h_a/h_s$.

Criterion R1. This parameter yields heat transfer augmentation (h_a/h_s) if smooth tubes are directly replaced by dimpled ones and flowrate remains unchanged. Due to the increase in pumping power, a pump replacement will usually be needed to implement this criterion.

If the log-mean temperature difference (LMTD) is assumed to be held constant, parameter R1 is calculated from $R1 = Nu_a/Nu_s$ where both Nusselt numbers are calculated for the same Reynolds numbers. Therefore, Criterion R1 directly yields the increase in Nusselt number shown in Fig. 10.

Nusselt number increase (R1) can be calculated from the relation between Nu_a (Eq. (13)) and Nu_s (Eq. (12)) having

$$R1 = 64.1(h/d)^{0.69}(d^2/pl)^{0.12}(Re - 1000)^{-0.21}. \quad (16)$$

Criterion R3. This parameter yields heat transfer augmentation (h_a/h_s) when smooth tubes are directly replaced by dimpled ones and pumping power is not increased. To keep pumping power constant the following equation has to be satisfied:

$$f_s Re_s^3 = f_a Re_a^3, \quad (17)$$

where Re_s is the equivalent smooth tube Reynolds number. Applying Blasius equation to obviate f_s, the equivalent smooth tube Reynolds number is given by:

$$Re_s = \left[\frac{f_a Re_a^3}{0.079}\right]^{0.364}. \quad (18)$$

Parameter R3 is calculated from the U_a/U_o relation, where $U_a \approx h_a$ is calculated at Re_a and $U_s \approx h_s$ is calculated at the equivalent Reynolds number Re_s. Heat transfer enhancement is only a function of Reynolds number.

As can be seen in Fig. 13, R3 decreases with an increase of Re_s for the whole Reynolds number range. At $Re_s = 4000$, heat transfer augmentation ranges from 70% to 110% ($R3 = 1.7$–2.1). At $Re_s = 10{,}000$, the value decreases to 1.5–1.7 and at $Re_s = 40{,}000$ heat transfer augmentation is only of 10–20%. The best performance is obtained for Tubes 03, 05 and 08 with the most reduced height, and better still for the tubes the minimum pitch (Tubes 03 and 05).

Criterion R5. This parameter yields the surface reduction obtained by a heat exchanger design if dimpled tubes are

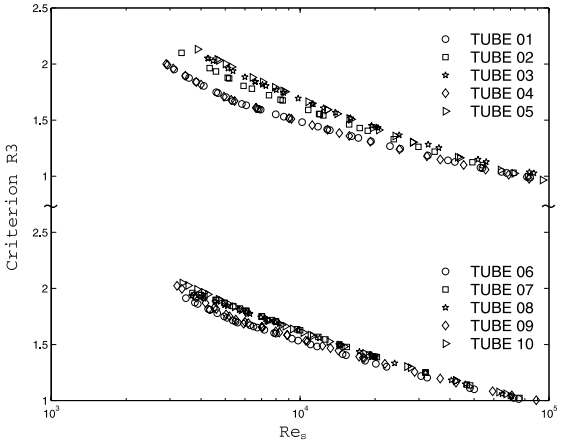

Fig. 13. R3 factor vs. Reynolds number.

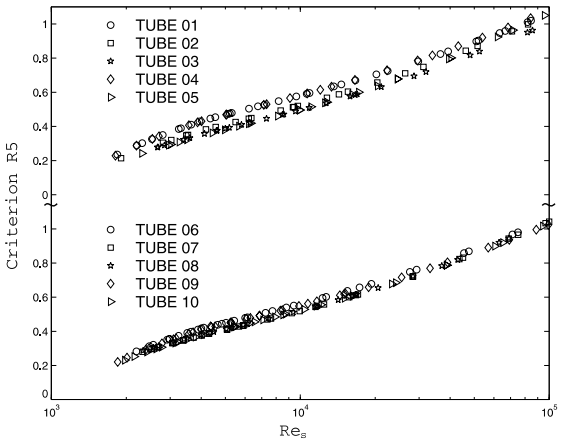

Fig. 14. R5 factor vs. Reynolds number.

used instead of smooth tubes. This surface reduction is determined for equal pumping power and heat duty.

Geometry is now variable, diameter is supposed to be constant and surface reduction can be obtained by reducing the number of tubes N, and/or tube length l. The equivalent smooth tube Reynolds number Re_s is obtained by:

$$f_s Re_s^3/Nu_s = f_a Re_a^3/Nu_a \Rightarrow Re_s^3 = \frac{f_a Re_a^3 Nu_s}{f_s Nu_a}. \quad (19)$$

f_a and Nu_a are calculated at a given Re_a by Eqs. (6) and (13), respectively. f_s and Nu_s are calculated by Eqs. (5) and (12). Re_s is calculated by an iterative method in Eq. (19). The relation between amounts of tubes N_a/N_s and their relative lengths l_a/l_s should be calculated in order to have a constant pumping power.

Results are shown in Fig. 14. As expected, $R5$ increases parallel to Re_s increase. At $Re_s = 4000$, the required surface can be reduced to 35–45% ($R5 = 0.35$–0.45). At $Re_s = 10{,}000$ $R5$ increases to 0.5–0.6 and at $Re_s = 40{,}000$ the required surface reaches about 80% of the required area, if smooth tubes were going to be used. From $Re = 80{,}000$ upwards, heat exchanger area would even be higher using dimpled tubes rather than smooth ones (according to Criterion R5).

6. Conclusions

1. All dimpled tubes showed higher pressure drop and heat transfer than the ones obtained for the smooth tube under the same flow conditions. Increases from 150% to 350% in friction factor coefficient and up to 250% in Nusselt number were observed.
2. General correlations were drawn so as to characterize this study's dimpled tube family. Reduced height h/d showed the highest influence in both f_a and Nu_a, whereas the effect of dimple density d^2/pl was relatively small.
3. The roughness function $R(h^+)$ was employed to correlate pressure drop results in the h^+ range 70–500. This correlation fits experimental friction factors within 5% of deviation. Heat transfer data were also correlated using the heat transfer roughness function $G(h^+, Pr)$. This correlation, together with $R(h^+)$ correlation, leads to a deviation within 7.5% for the calculated Nusselt number.
4. Measurements were taken at 5 fixed Prandtl numbers (2.9, 4.1, 37, 59 and 92) in order to accurately establish Pr influence on heat transfer. Results showed the same Pr influence for the smooth tube as for all dimpled tubes, $Nu \propto Pr^{0.4}$. Therefore, both dimpled tube heat transfer augmentation and performance criterion are non-dependent on Pr.
5. According to performance evaluation Criteria R3 and R5 suggested by Bergles et al. [1], the deeper the dimple (higher h/d), the better the performance. The performance study shows that dimpled tubes are suitable for Re ranging between 2000 and 40,000. Heat transfer increases from 20% to 110% can be obtained if smooth tubes are replaced by dimpled ones, following Criterion R3. In a heat exchanger design, the total area can be reduced from 80% to 20% if dimpled tubes are used instead of smooth ones (R5 criterion).
6. This study contributes to lessen the lack of experimental data on three dimensional roughness, currently observed. The family of dimpled tubes with similar geometry to those studied in the current work have been characterized. Correlations obtained for pressure drop and heat transfer can be directly employed for design purposes, with a high level of accuracy under a wide range of flow conditions: $Re = 2000$–$100{,}000$ and $Pr = 2.5$–100.

Acknowledgements

This research has been partially financed over the 1FD1997-0211 (TYP) grant of the "Dirección General de Enseñanza Superior e Investigación Científica" in Spain and the HRS Spiratube company from Murcia (Spain).

References

[1] A.E. Bergles, A.R. Blumenkrantz, J. Taborek, Performance evaluation criteria for enhanced heat transfer surfaces, Heat Transfer 2 (1974) 239–243.
[2] R.L. Webb, Principles of Enhanced Heat Transfer, first ed., Wiley/Interscience, New York, 1994, p. 556.
[3] W.G. Cope, The friction and heat transmission coefficients of rough pipes, Proc. Inst. Mech. Eng. 145 (1945) 99–105.

[4] D.F. Dipprey, R.H. Sabersky, Heat and momentum transfer in smooth and rough tubes at various Prandtl numbers, Int. J. Heat Mass Transfer 6 (1963) 329–353.
[5] K. Takahashi, W. Nakayama, H. Kuwahara, Enhancement of forced convective heat transfer in tubes having three-dimensional spiral ribs, Heat Transfer – Jpn. Res. 17 (1988) 12–28.
[6] L. Cuangya, G. Chuanyun, W. Chaosu, H. Jinshu, J. Cun, Experimental investigation of transitional flow heat transfer of three-dimensional internally finned tubes, in: Advances in Heat Transfer Augmentation and Mixed Convection, ASME Symposium, HTD-169, 1991, pp. 45–48.
[7] H. Kuwakara, K. Takahashi, T. Yanagida, T. Nakayama, S. Hzgimoto and K. Oizumi, Method of producing a heat transfer tube for single phase-flow, US Patent 4,794,775, (1989).
[8] T.J. Rabas, R.L. Webb, P. Thors, N.K. Kim, Influence of roughness shape and spacing on the performance of three-dimensional helically dimpled tubes, J. Enhanced Heat Transfer 1 (1993) 53–64.
[9] R.P. Taylor, B.K. Hodge, Fully developed heat transfer and friction factor predictions for pipes with three dimensional roughness, in: Fundamentals of Forced Convection Heat Transfer, ASME Symposium, HTD-210, 1992, pp. 75–84.
[10] C.O. Olsson, B. Sundén, Heat transfer and pressure drop characteristics of 10 radiator tubes, Int. J. Heat Mass Transfer 39 (1996) 3211–3220.
[11] W.J. Marner, A.E. Bergles, J.M. Chenoweth, On the presentation of performance data for enhanced tubes used in shell-and tube heat exchangers, J. Heat Transfer 105 (1983) 358–365.
[12] R. Sethumadhavan, M.R. Rao, Turbulent flow friction and heat transfer characteristics of single and multistart spirally enhanced tubes, J. Heat Transfer 108 (1986) 55–61.
[13] W.M. Kays, A.L. London, Compact Heat Exchangers, third ed., McGraw-Hill, New York, 1984.
[14] A. Bejan, Heat Transfer, first ed., Wiley, New York, 1984.
[15] S.J. Kline, F.A. McClintock, Describing uncertainties in single sample experiments, Mech. Eng. 75 (1953) 3–8.
[16] J. Nikuradse, Laws of flow in rough pipes, VDI Forschungsheft, 1933, p. 361 (English translation, NACA TM-1292, 1965).
[17] R.L. Webb, R.G. Eckert, R.J. Goldstein, Heat transfer and friction in tubes with repeated-rib roughness, Int. J. Heat Mass Transfer 14 (1971) 601–617.
[18] V.D. Zimparov, N.L. Vulchanov, L.B. Delov, Heat transfer and friction characteristics of spirally corrugated tubes for power plant condensers. 1. Experimental investigation and performance evaluation, Int. J. Heat Mass Transfer 34 (1991) 2187–2197.
[19] L.J. Brognaux, R.L. Webb, L.M. Chamra, Single phase heat transfer in micro-fin tubes, Int. J. Heat Mass Transfer 40 (1997) 4345–4357.
[20] V. Gnielinski, New equations for heat and mass transfer in turbulent pipe and channel flow, Int. Chem. Eng. 16 (1976) 359–368.
[21] B.S. Petukhov, Heat transfer and friction in turbulent pipe flow with variable physical properties, in: Advances in Heat Transfer, vol. 6, Academic Press, New York, 1970, pp. 503–564.
[22] R.L. Webb, Performance evaluation criteria for use of enhanced heat transfer surfaces in heat exchanger design, Int. J. Heat Mass Transfer 24 (1981) 715–726.